

# Age and geochemistry of lithospheric mantle underlying Marie Byrd Land, Antarctica

Adam McKeeby  
April 10, 2015

Dr. Richard Walker and Dr. Phil Piccoli  
GEOL394

## Contents

Abstract.....	4
1. Introduction.....	4
2. Geological Background .....	6
3. Analytical Methods.....	6
3.1 Sample preparation .....	6
3.2 Mineral compositions.....	6
3.3 Whole rock major and trace elements.....	7
3.4 Isotope Dilution and Measurement of Osmium.....	7
3.5 Isotope Dilution and Measurement of Re .....	7
4. Results.....	8
4.1 Mineral chemistry .....	8
4.2 Whole rock major and trace elements.....	9
4.3 Osmium isotopes.....	9
5.0 Discussion .....	10
5.1 Age of the lithospheric mantle .....	10
6. Conclusions.....	11
Suggestions for future work .....	11
Appendix.....	12
Table 1-Re-Os isotopic data and selected major elements.....	12
Table 2-Summary of Average Major Element Composition of Olivine.....	13
Table 3- Summary of XRF Major and Minor Elements .....	14
Table 4-Summary of XRF vs EPMA Mg# data.....	15
References.....	16

## Abstract

The mineral compositions, whole rock major and trace elements concentrations, and Re–Os isotopes of 18 peridotite xenoliths from Marie Byrd Land Antarctica were determined in order to constrain the structure and evolution of the upper lithospheric mantle. Re–Os isotope measurements are used to determine model ages for the melting of the rocks. Electron probe microanalysis is used to determine compositions of the major minerals olivine to examine the melting history of samples.

Samples are from four Cenozoic alkaline volcanic centers. The peridotite xenolith samples were entrained in a basaltic host rock from these four centers. The peridotites are generally fertile (e.g., 89.2–92.9 with an average of  $90.1 \pm 2(2\sigma)$ ). Proterozoic lithosphere stabilization model ages of ca. 1.1 and  $>1.3$  Ga are recorded in xenoliths from past studies. The Mesoproterozoic Os model ages are consistent with Proterozoic Nd model ages in Marie Byrd Land granites and orthogneisses, and with a zircon age of 1.1 to 1.5 Ga in the thick Swanson Formation sediments that are exposed along the coast (Pankhurst et al. 1998). Most of the peridotites in this study have TRD model ages of late Proterozoic (.9 Ga–1.17 Ga) to Cambrian (.45–.59 Ga), suggesting that the lithospheric mantle underlying the crust is approximately the same age as the overlying crust of Marie Byrd Land. This also may indicate that the original Mesoproterozoic mantle lithosphere has been conformed with the overlying crust.

## 1. Introduction

The study of upper lithospheric mantle peridotite xenoliths entrained in alkaline magmas from the West Antarctic Rift System has produced information on the composition and processes within the upper mantle and lower crust. Rhenium–Osmium isotopic systematics can constrain the time of melt depletion events in the peridotites using Os model ages (Rudnick and Walker, 2009). This method operates under the assumption that lithosphere formation happens at the same time with melt depletion. The Re–Os system can be used to constrain the time of lithosphere stabilization through the use of model ages that estimate the timing of melt extraction in the mantle and isolation of the residue in the lithosphere. This system works because of the difference in bulk partition coefficients between Re relative to Os. Re is relatively incompatible, with a lower bulk partition coefficient whereas Os has a larger bulk partition coefficient. Therefore during partial melting Re is separated from Os. This causes Re/Os ratios to be high in melts, and low in the residual rock (Rudnick et al., 2009). This is the basis for the Re–Os chronometers.

The two Re–Os model ages being calculated are  $T_{MA}$  and TRD model ages.  $T_{MA}$  references the  $^{187}\text{Os}/^{188}\text{Os}$  isotopic composition evolution of residual peridotite to a model curve that represents a chondritic upper mantle evolution, using the measured Re/Os value of the samples.  $T_{MA}$  model ages typically are generally not useful for peridotite xenoliths because of the mobility of Re which causes changes measured Re/Os values, usually by the addition from the host basalt that the xenolith is entrained in (Walker et al., 1989). This method relies on knowing the Re that moved into the melt. Instead of  $T_{MA}$ , redepletion model ages (TRD: Walker et al., 1989) are typically used for individual peridotite xenoliths from cratonic regions. TRD model ages differ from  $T_{MA}$  ages in that they are independent of ingrowth of Os due to Re values and assume all Re has been extracted during melting. Therefore they can only provide minimum time estimates of melt depletion events, which are the shortest lengths of time that the events could possibly have occurred (e.g. Walker et al., 1989; Pearson et al., 1995). If samples have

undergone large degrees of melt extraction, then they will provide the tightest constraints on the time estimates since more Re would have left the residue, and therefore the assumption of near-complete Re removal during melt extraction becomes more reasonable. Therefore, TRD model ages are more viable for these samples, since the initial abundance of Re before melting cannot be measured (Walker et al., 1989).

The Re–Os isotopes in peridotite are relatively resistant to metasomatic overprinting and have been used to date melt depletion events in mantle peridotites (e.g., Walker et al., 1989, Handler et al., 1997, Handler et al., 2003). Most applications of Re–Os dating rely on comparisons of the isotopic compositions of samples with mantle evolution models. Re–Os model ages are sensitive to the degree to which the samples have followed the simplified mantle evolution models used to calculate the age (Rudnick and Walker, 2009). Dating melt depletion events recorded in peridotites from the lithospheric mantle and the formation of the lithospheric mantle is important for understanding the relationship and dynamics between the lithospheric mantle and overlying crust. The prevailing hypotheses for the lithosphere under Marie Byrd Land, Antarctica are 1) the overlying crustal block may have tectonically overridden lithosphere of the East Antarctic Craton (Handler et al. 2003), 2) that the lithosphere beneath it is a fragment of continental lithospheric mantle that originated in the oceanic lithosphere during rifting and break up of Rodinia where the piece of mantle lithosphere delaminated off another piece and accreted to the Antarctic margin (Hassler and Shimizu, 1998) . The older lithosphere could possibly have come from eastern Antarctica as well. These hypotheses are based on the changes to the lithospheric mantle during continental break up, subduction, accretion processes, and convection within the mantle. In this study, the Hannuoba region in the North China Craton (NCC) is used for comparison. In the case of the NCC, the lithospheric mantle was found to not have the same age as the crust. The crust was formed in the Archean (~2.5 Ga) and the results of the Liu et al. (2012) study suggested that there was lithospheric mantle removal and replacement during the Paleoproterozoic (~1.8 Ga). Also this study will be compared to Handler et al. (2003) study, which concluded that the lithospheric mantle underneath Marie Byrd Land co-formed with the overlying crust, and both are relatively similar in model ages of 1.1-1.3 Ga and 1.1-1.5 Ga (Pankhurst et al. 1998) respectively.

Here I provide results from a Re–Os isotopic study, major and trace element geochemistry of a peridotite xenolith suite from Marie Byrd Land. The 18 samples in the suite were acquired from Christine Siddoway of Colorado College and Chris Yakymchuck of the University of Maryland. The samples were brought to the surface by Cenozoic alkaline volcanism.

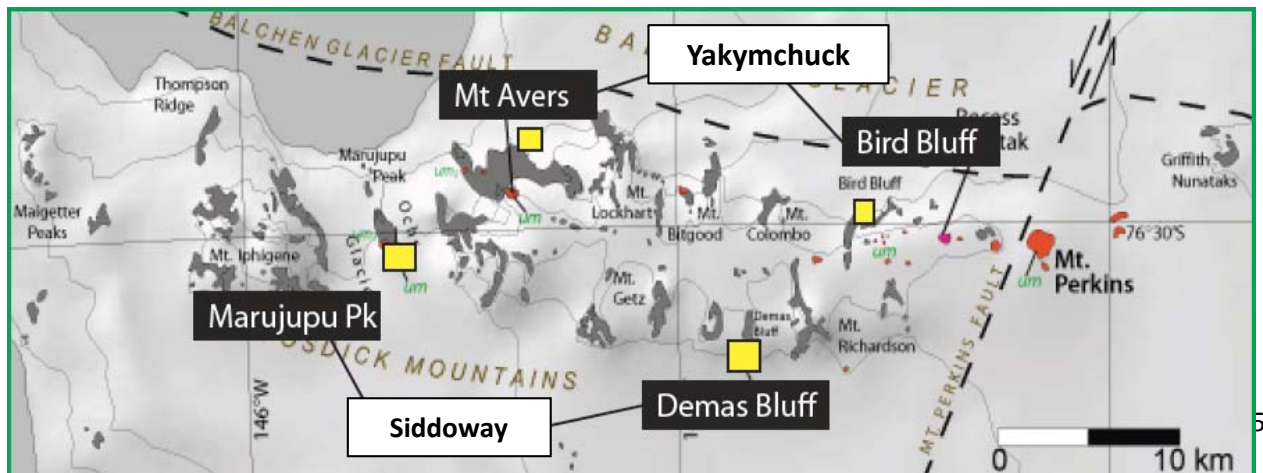


Figure 1: The Fosdick Mountains in Marie Byrd Land, Antarctica. Sample locations are indicated by the labels and their corresponding lines. Siddoway and Yakymchuck, were the two people who acquired the samples

## 2. Geological Background

Marie Byrd Land is one of several allochthonous crustal blocks that compose the continental assemblage of the East Antarctic craton. In combination with eastern Australia and western New Zealand, West Antarctica was part of the paleo-Pacific margin of Gondwana until break-up during the Mesozoic approximately 100 Ma (Lawver et al., 1991). Episodes of convergence and divergence have affected the region since Jurassic times (Wysoczanski et al., 1995). Outcrops usually consist of thick Cambrian-Ordovician turbidite sediments and intrusions of granitoids (Handler et al., 2003). Generally, it is very difficult to observe much exposure of crustal rocks anywhere but the coastal and near-coastal area due to the large amount of sheet ice covering the continent. The oldest exposed rocks in the upper crust are 500 Ma orthogneisses in eastern Marie Byrd Land. The oldest exposed sediments found in West Antarctica are 1.1-1.5 Ga, derived from Sm-Nd model ages from detrital zircons (Pankhurst et al. 1998). The source of these sediments is thought to be from the Ross-Delamerian orogenic belt which is exposed in west Antarctica (Ireland et al., 1994). Lower crustal xenoliths from Cenozoic volcanoes indicate that the lower crust beneath Marie Byrd Land is composed of meta-igneous cumulate pyroxenites, gabbros, and norites of varying composition. Geochemical studies indicate that the lower crust is moderately primitive in composition, and evolved silicic crust is entirely absent (Wysoczanski et al., 1995).

Marie Byrd Land is also undergoing extension currently. During Cretaceous times, the tectonics transitioned from convergent to extensional. It is thought that this was either caused by the arrival of a plume under Ross Island (Storey et al. 1999), or due to a ridge-trench interaction (Mukasa and Dalziel, 2000). This extensional environment resulted in the opening of the West Antarctic Rift System, which stretches approximately 3000 km across the edge of Marie Byrd Land, and the separation of New Zealand from the Gondwana margin (Handler et al., 2003).

## 3. Analytical Methods

### 3.1 Sample preparation

Thin sections of each xenolith collected from the suite were analyzed in order to assess the range in degree of melt depletion. Portions of the samples were first cut into billets and then sent to Texas Petrographics for the preparation of thin sections for each sample. Olivine and pyroxene compositions in the sections were determined using a JEOL 8900 Electron Probe Microanalyzer (EPMA) at the University of Maryland. Remaining portions of each sample were powdered for whole rock analyses and isotope dilution.

### 3.2 Mineral compositions

Major element compositions of olivine, orthopyroxene, and clinopyroxene were determined on the polished thin sections by EPMA at the University of Maryland. The analyses, of each thin section, were performed by using wavelength dispersive spectroscopy. Naturally formed olivines and pyroxenes were used as standards. 2 spots per grain and 5-10 grains per mineral phase were analyzed per sample. These data were then used to find forsterite content ( $Fo = Mg/(Mg+Fe^{2+}) \times 100$ ) of olivines. Analytical uncertainties were typically under 0.5% for the major elements for olivine and under 0.4% for pyroxenes.

### 3.3 Whole rock major and trace elements

Whole rock major element compositions were determined by X-ray fluorescence (XRF) on fused disks made from powders at Franklin and Marshall College (see Boyd and Mertzman (1987) for procedure). Analytical error was usually better than 1% ( $1\sigma$ ) for the major elements of concentrations greater than 1%( $1\sigma$ ) and better than 5% ( $1\sigma$ ) for the remaining major elements.

### 3.4 Isotope Dilution and Measurement of Osmium

Isotope dilution is used to find the ratio of isotopes of a particular element. Isotope dilution is adding spike solution (with a known ratio of the same isotopes, but enriched in the minor isotope) to a solution with an unknown ratio of isotope system with a natural isotope composition (the sample). After isotope equilibration, the isotope composition in the mixture is measured by mass spectrometry.

In this study, mixed  $^{185}\text{Re}$ - $^{190}\text{Os}$  and Highly Siderophile Element ( $^{99}\text{Ru}$ ,  $^{105}\text{Pd}$ ,  $^{191}\text{Ir}$ ,  $^{194}\text{Pt}$ ) spikes were added to each sample powder (1–1.5 g), sealed along with 2 ml concentrated Teflon distilled HCl and 4 ml concentrated Teflon distilled HNO<sub>3</sub> into a chilled, Carius tube, and heated to 270 °C for 3 days. Osmium was extracted from the acid solution using CCl<sub>4</sub>, which was then separated from the acid and then back-extracted into HBr. The CCl<sub>4</sub> is then removed and the HBr solution is then dried down. The remaining dried down Os is finally purified via microdistillation. Microdistillation is done by adding dichromate on top of the dried sample, and trapping the re-oxidized Os in a small drop of HBr suspended in a small sealed Teflon vessel. The Teflon vessel is then subsequently wrapped in aluminum foil and heated to 80° C for 2-3 hours. The HBr is then dried down to yield clean Os metal. If appeared to be residue other than Os metal, then microdistillation was run again till clean.

Osmium isotopic measurements were performed by negative thermal ionization mass spectrometry (N-TIMS) at the University of Maryland. All samples were measured using VG Sector 54 or NBS mass spectrometers. The precision on the  $^{187}\text{Os}$ / $^{188}\text{Os}$  was typically better than 0.1%. In order to run the mass spectrometers, the samples had to be loaded onto filaments to put into the mass spectrometers. This was done by adding 1.6 microliters of HBr to the Os metal to dissolve. Then .9 microliters of that solution is added on top and center of platinum filaments, and then dried by running a low current through the filament. Then enough Ba(OH)<sub>2</sub> is added to lightly coat the entire top of the filament. The filament is dried again by running a low current through it. Once that is dried, indicated by a white coat on top of the filament, the current is increased slowly to melt the Ba(OH)<sub>2</sub>. It is then dried again. At this point it is loaded into the mass spectrometer.

### 3.5 Isotope Dilution and Measurement of Re

After Os separation is finished, the remaining sample needs to be centrifuged for 5-10 minutes. Immediately following that, pipette the aqua regia solution into a 15 ml beaker for drying. Avoid pipetting any of the solid in the centrifuge. Dry down till it is highly viscous but, not completely dry. Once dried to the viscous solution add 2.5 ml 1 N TD HCl and place on a hot plate at 80° C overnight. The following day, put the solution back into a centrifuge tube and centrifuge again for 5-10 minutes. The solution is then ready for column elution. There are two column elutions. The first and primary column separates out the Re from solution. The second is

to further purify the Re. After both columns are finished the Re(dissolved in 7 ml 6N HNO<sub>3</sub>) will be dried down. When it is dried down, it is then redissolved in 5% HNO<sub>3</sub>. Once the solution is dissolved, they can be run through the ICP-MS.

## 4. Results

### 4.1 Mineral chemistry

The average forsterite contents of olivines analyzed in grain mounts for the xenoliths are plotted as histograms in Figure 2. My samples are characterized by a range of Fo from 89.2-92.1 with an average of  $90.1 \pm 2(2\sigma)$ . By comparison, the Hannuoba samples have a range of 87.4-92.2 with an average of  $90.5 \pm 5(1\sigma)$  (Liu et al., 2011). Figure 2 shows that the samples appear to

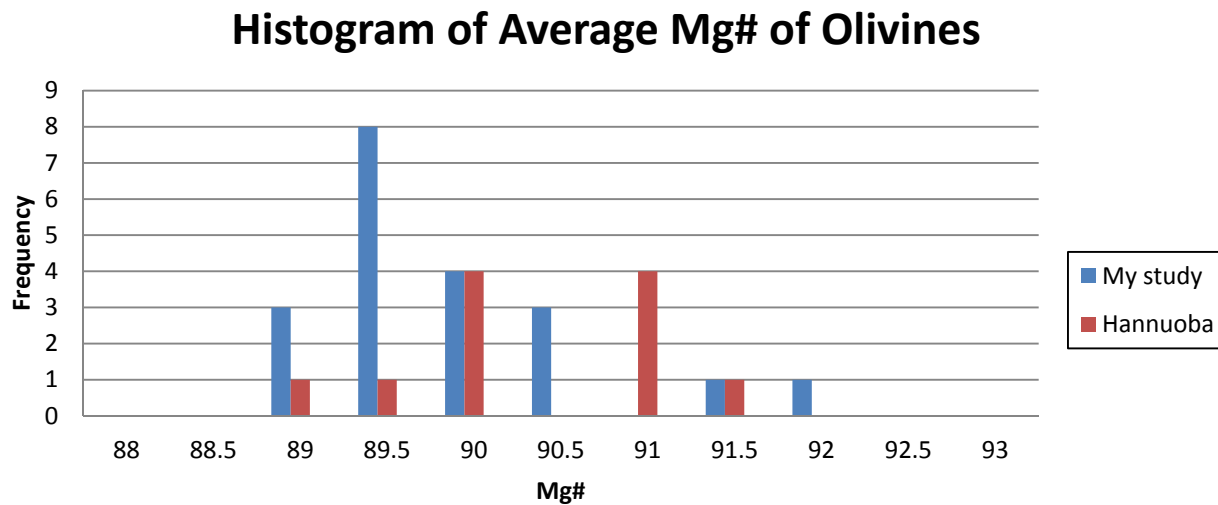


**Figure 2.** Hannuoba is from the northern part of the NCC. Liu et al. (2011) concluded that Hannuoba has younger lithospheric mantle relative to the overlying crust.

be similar to the Hannuoba samples. The lower Fo reflects more fertile samples and the higher Fo reflect more refractory samples. The majority of the data from this study indicate that the source is more fertile than refractory, indicating a more fertile lithospheric mantle underlying this region of Marie Byrd Land.

## 4.2 Whole rock major and trace elements

The peridotites show poor to moderate correlation on the plot of  $^{187}\text{Os}/^{188}\text{Os}$  vs.  $\text{Al}_2\text{O}_3$ . Correlations between and  $\text{Al}_2\text{O}_3$  are interpreted to reflect melt depletion (Rudnick and Walker, 2009). The majority of the samples are relatively fertile, which is supported by both the whole rock Fo and the Fo of olivine. These samples have  $\text{Al}_2\text{O}_3$  contents from 1.12%-4.09%. The  $\text{Al}_2\text{O}_3$  contents do not go below 1% in any of the samples. This is noteworthy because the general marker for complete Re removal for melt depletion is analogous to an  $\text{Al}_2\text{O}_3$  content of 0.7% or less, which is essential for the TRD model ages used in this study. This is because  $\text{Al}_2\text{O}_3$  has a similar bulk partition coefficient to Re, which  $\text{Al}_2\text{O}_3$  can serve as a proxy for Re (Rudnick and Walker, 2009).

## 4.3 Osmium isotopes

Whole rock Os isotopes are reported in Table 1 in the appendix. The majority of the data is younger than the overlying crust and grouped within .45-.59 Ga, which is closer to the ages of

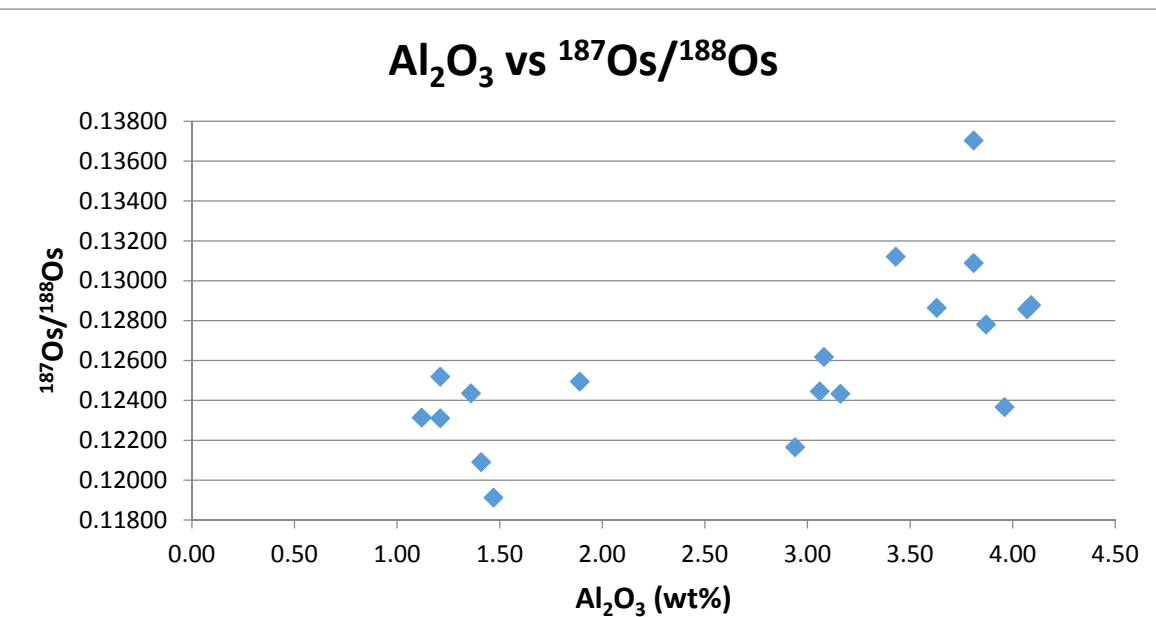


**Figure 3:** As partial melting increases  $\text{Al}_2\text{O}_3$  weight percentage will decrease. These data show a poor-moderate positive correlation. The data with the lower  $\text{Al}_2\text{O}_3$  weight percentage is older than that with higher percentage lithospheric mantle, suggested by Handler et al. (2003), which had ages of 0.9 and 1.17 Ga. This is important because TRD model ages are meant to provide a minimum estimate of melt depletion age. This gives ages consistent with oldest ages found in Handler et al. (2003) within the Mesoproterozoic.

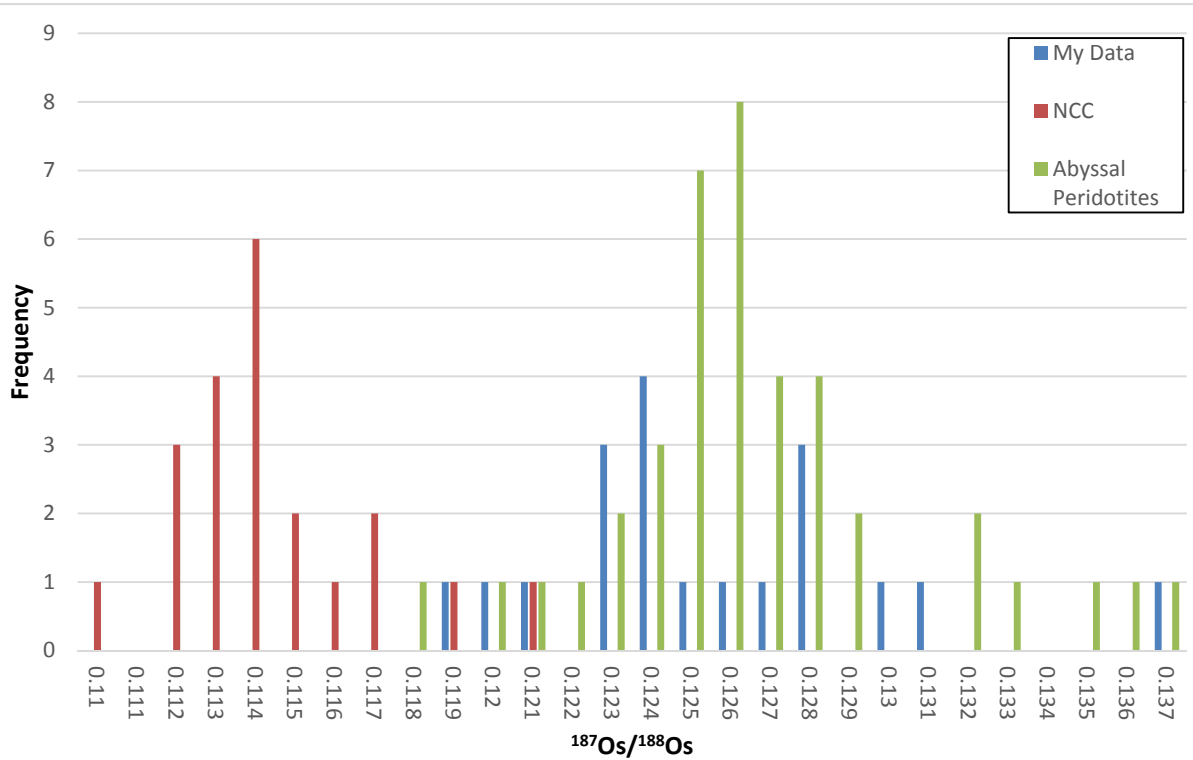


**Figure 4.** Histograms of  $^{187}\text{Os}/^{188}\text{Os}$  of whole rock peridotites from the southern NCC (Red), my study (blue) and abyssal peridotite data (green) from North Korea. The peaks of the three sets of data indicate the most frequent  $^{187}\text{Os}/^{188}\text{Os}$  ratio and therefore the most frequent  $T_{\text{RD}}$  model age. Abyssal peridotites have more samples in higher ratios, and the southern NCC has the lower ratios. As  $^{187}\text{Os}/^{188}\text{Os}$  ratio decreases so does the  $T_{\text{RD}}$  model age. The oldest model age from my data is 1.17 Ga.

## 5.0 Discussion

### 5.1 Age of the lithospheric mantle

The results found by Handler et al. (2003) suggested that the lithospheric mantle had a model age of 1.1-1.3 Ga underneath Marie Byrd Land. This study has evidence agreeing that there was possibly a melt depletion event occurred at the model age of .9 Ga-1.17 Ga in the lithospheric mantle underneath Marie Byrd Land. This is derived from  $^{187}\text{Os}/^{188}\text{Os}$  data peaks on Figure 4 between .118 and .12, which correspond with 1.17 Ga and .9 Ga model ages respectively. These data are further supported by data with younger model ages in Figure 4, where the peak distribution is more in line with the peak distribution of abyssal peridotites, instead of being closer to the much older Archean aged peridotites from the southern NCC. These model ages are within uncertainty of the age of the crust. The whole rock and olivine data also suggest that there was enough partial melting to have Re mobilized for the  $T_{\text{RD}}$  model age to be a valid model.

## 6. Conclusions

These data indicate that the lithospheric mantle underneath Marie Byrd Land underwent a melt depletion event near within the same model age range as the overlying crust (1.1-1.5 Ga). Furthermore, this would suggest that the both the crust and lithospheric mantle present today were co-formed, that the lithospheric mantle that formed during the formation of the crust has since been removed. The TRD model ages may be a good indicator of the lithospheric mantle currently under the Fosdick Mountains, due to the negative correlation of  $\text{Al}_2\text{O}_3$  weight percent and  $^{187}\text{Os}/^{188}\text{Os}$ , which indicates melt depletion has occurred. This is essential for the model to work, as enough melt depletion is needed to mobilize Re into a leaving residue. These data are within the uncertainties of the Handler et al. (2003) study to suggest a similar model age for the lithospheric mantle beneath Marie Byrd Land. This indicates co-formation of the mantle lithosphere and the overlying crust.

## Suggestions for future work

Further work on these samples could include finding the Highly Siderophile elements abundances (HSE) to determine the effects of secondary processes that may have affected the amount of Os or Re present, which would ultimately change what the  $T_{\text{RD}}$  model age was of the samples. Also 18 samples is a relatively small suite in comparison to similar studies, like Liu et al. (2011) where there were over 300 peridotites used in their analysis, which could further support any model age determinations. Also important was the distribution of samples across the NCC. If something were done similarly, especially between the Fosdick Mountains (my study) and the Executive Ranges (Handler et al., 2003), this could potentially give a more clear interpretation of the age of the lithospheric mantle underneath Marie Byrd Land, or more interestingly may suggest that there is a lithospheric boundary in between the two locations.

## Appendix

Data for all olivine major element analysis from the EPMA and whole rock data, for individual samples, from the XRF are available upon request through an electronic file.

**Table 1-Re-Os isotopic data and selected major elements**

Sample	Location	Sample Weight	Al <sub>2</sub> O <sub>3</sub> (Wt. % Whole Rock)	Re (ppb)	Os (ppb)	<sup>187</sup> Os/ <sup>188</sup> Os	<sup>187</sup> Re/ <sup>188</sup> Os	T <sub>MA</sub> (Yr)	T <sub>RD</sub> (Ga)
2.1	Demas Bluff	1.55	1.47	0.058	3.3171	0.11912	0.084	1.49E+09	1.17
6.1	Demas Bluff	1.51	1.12	0.054	1.2868	0.12313	0.202	1.18E+09	0.57
6.2	Demas Bluff	1.54	1.41	0.039	1.8722	0.12091	0.100	1.22E+09	0.90
8.1	Demas Bluff	1.50	1.89	0.151	2.0888	0.12494	0.348	2.37E+09	0.31
11.1	Demas Bluff	1.50	1.21	0.165	2.5588	0.12519	0.310	1.24E+09	0.27
11.1(repeat)	Demas Bluff	1.50	1.21	0.027	0.5808	0.12310	0.223	1.33E+09	0.58
4.1	Marujupo Peak	1.50	1.36	0.011	0.5579	0.12435	0.096	5.36E+08	0.39
7.1	Marujupo Peak	1.51	3.06	0.123	1.9412	0.12445	0.304	1.61E+09	0.38
9.1	Marujupo Peak	1.51	2.94	0.050	1.1264	0.12165	0.213	1.71E+09	0.79
AVX 18	Mt. Avers	1.50	3.08	0.122	1.7639	0.12618	0.333	8.00E+08	0.12
AVX 20	Mt. Avers	1.50	3.81	0.046	2.6077	0.13704	0.085	-1.91E+09	-1.52
AVX 25	Mt. Avers	1.57	3.87	0.052	1.6523	0.12781	0.151	-1.69E+08	-0.12
AVX 27	Mt. Avers	1.51	3.63	0.009	1.6857	0.12864	0.026	-2.47E+08	-0.25
AVX 28	Mt. Avers	1.51	3.81	0.147	2.4330	0.13089	0.290	-2.08E+09	-0.58
AVX 29	Mt. Avers	1.51	3.16	0.150	3.1659	0.12433	0.228	9.47E+08	0.40
AVX 30	Mt. Avers	1.51	4.07	0.061	2.0899	0.12857	0.140	-3.39E+08	-0.24
BBX 16	Bird Bluff	1.50	3.96	0.075	1.7827	0.12367	0.204	1.03E+09	0.50
BBX 18	Bird Bluff	1.50	3.43	0.148	1.7358	0.13121	0.411	2.15E+10	-0.63
BBX 22	Bird Bluff	1.51	4.09	0.093	1.3137	0.12878	0.342	-1.71E+09	-0.27

**Table 2-Summary of Average Major Element Composition of Olivine**

<b><i>Location</i></b>	<b><i>Sample</i></b>	<b><i>MgO</i></b>	<b><i>SiO<sub>2</sub></i></b>	<b><i>FeO</i></b>	<b><i>NiO</i></b>	<b><i>MnO</i></b>	<b><i>Mg#</i></b>
Demas Bluff	2.1	50.71	40.57	8.15	0.41	0.11	91.7
Demas Bluff	6.1	49.24	40.50	10.22	0.35	0.15	89.6
Demas Bluff	6.2	48.85	40.67	10.12	0.35	0.15	89.6
Demas Bluff	8.1	49.17	40.67	9.51	0.35	0.14	90.2
Demas Bluff	11.1	51.00	40.82	7.80	0.40	0.11	92.1
Marujupo Peak	4.1	49.34	40.87	9.51	0.37	0.15	90.2
Marujupo Peak	7.1	50.09	40.59	9.09	0.39	0.12	90.8
Marujupo Peak	9.1	49.89	40.69	9.04	0.38	0.13	90.8
Mt. Avers	AVX 18	49.28	41.03	9.56	0.38	0.13	90.2
Mt. Avers	AVX 20	48.53	40.37	10.07	0.39	0.15	89.6
Mt. Avers	AVX 25	47.15	40.44	10.00	0.41	0.12	89.4
Mt. Avers	AVX 27	48.68	40.55	9.91	0.41	0.13	89.8
Mt. Avers	AVX 28	48.64	40.21	10.00	0.40	0.14	89.7
Mt. Avers	AVX 29	49.17	40.71	9.36	0.40	0.14	90.3
Mt. Avers	AVX 30	48.71	40.33	9.89	0.41	0.14	89.8
Bird Bluff	BBX 16	48.98	40.75	10.24	0.40	0.14	89.5
Bird Bluff	BBX 18	48.96	40.64	10.19	0.40	0.13	89.5
Bird Bluff	BBX 22	48.30	40.63	10.26	0.40	0.14	89.4

**Table 3- Summary of XRF Major and Minor Elements**

<b>Location</b>	<b>MgO</b>	<b>SiO<sub>2</sub></b>	<b>Fe<sub>2</sub>O<sub>3</sub>T</b>	<b>Al<sub>2</sub>O<sub>3</sub></b>	<b>CaO</b>	<b>MnO</b>	<b>Na<sub>2</sub>O</b>	<b>TiO<sub>2</sub></b>	<b>K<sub>2</sub>O</b>	<b>P<sub>2</sub>O<sub>5</sub></b>	<b>TOTAL</b>	<b>WR Mg#</b>
Demas Bluff	44.30	43.40	8.63	1.47	0.85	0.14	0.14	0.05	0.03	0.04	99.05	90.148
Demas Bluff	44.91	43.83	8.30	1.12	0.59	0.14	0.10	0.02	0.01	0.02	99.04	90.606
Demas Bluff	45.00	42.69	8.35	1.41	0.87	0.14	0.32	0.17	0.10	0.07	99.11	90.572
Demas Bluff	40.85	44.94	8.47	1.89	1.26	0.15	0.57	0.36	0.19	0.10	98.77	89.580
Demas Bluff	44.67	44.18	8.04	1.21	0.59	0.14	0.09	0.01	0.01	0.02	98.96	90.829
Marujupo Peak	45.14	42.99	8.71	1.36	0.87	0.14	0.23	0.12	0.06	0.05	99.68	90.233
Marujupo Peak	40.01	44.26	8.73	3.06	2.30	0.15	0.25	0.09	0.01	0.02	98.88	89.094
Marujupo Peak	40.13	43.82	9.34	2.94	2.16	0.15	0.29	0.12	0.03	0.03	99.01	88.451
Mt. Avers	40.34	43.62	9.26	3.08	2.84	0.15	0.30	0.09	0.01	0.02	99.70	88.592
Mt. Avers	38.95	43.56	9.67	3.81	3.00	0.15	0.37	0.12	0.02	0.02	99.67	87.775
Mt. Avers	39.42	43.39	9.26	3.87	3.27	0.16	0.34	0.12	0.02	0.02	99.87	88.357
Mt. Avers	37.94	44.53	8.96	3.63	3.57	0.15	0.35	0.12	0.01	0.02	99.28	88.302
Mt. Avers	37.75	44.36	8.96	3.81	3.57	0.15	0.39	0.15	0.01	0.02	99.16	88.250
Mt. Avers	40.50	43.22	9.03	3.16	2.86	0.15	0.29	0.09	0.01	0.02	99.33	88.883
Mt. Avers	37.87	44.29	9.11	4.07	3.32	0.15	0.35	0.14	0.01	0.02	99.33	88.110
Bird Bluff	38.84	43.02	9.59	3.96	3.54	0.15	0.35	0.12	0.06	0.02	99.64	87.834
Bird Bluff	40.68	42.04	10.03	3.43	2.64	0.16	0.25	0.10	0.06	0.02	99.41	87.849
Bird Bluff	37.66	44.10	9.06	4.09	4.00	0.15	0.37	0.14	0.05	0.02	99.63	88.109

**Table 4-Summary of XRF vs EPMA Mg# data**

	Location	Whole Rock			Olivine		
		MgO	Fe <sub>2</sub> O <sub>3</sub> T	Mg#	MgO	FeO	Mg#
2.1	Demas Bluff	44.30	8.63	90.1	50.71	8.15	91.7
6.1	Demas Bluff	44.91	8.30	90.6	49.24	10.22	89.6
6.2	Demas Bluff	45.00	8.35	90.6	48.85	10.12	89.6
8.1	Demas Bluff	40.85	8.47	89.6	49.17	9.51	90.2
11.1	Demas Bluff	44.67	8.04	90.8	51.00	7.80	92.1
4.1	Marujupo Peak	45.14	8.71	90.2	49.34	9.51	90.2
7.1	Marujupo Peak	40.01	8.73	89.1	50.09	9.09	90.8
9.1	Marujupo Peak	40.13	9.34	88.5	49.89	9.04	90.8
AVX 18	Mt. Avers	40.34	9.26	88.6	49.28	9.56	90.2
AVX 20	Mt. Avers	38.95	9.67	87.8	48.53	10.07	89.6
AVX 25	Mt. Avers	39.42	9.26	88.4	47.15	10.00	89.4
AVX 27	Mt. Avers	37.94	8.96	88.3	48.68	9.91	89.8
AVX 28	Mt. Avers	37.75	8.96	88.2	48.64	10.00	89.7
AVX 29	Mt. Avers	40.50	9.03	88.9	49.17	9.36	90.3
AVX 30	Mt. Avers	37.87	9.11	88.1	48.71	9.89	89.8
BBX 16	Bird Bluff	38.84	9.59	87.8	48.98	10.24	89.5
BBX 18	Bird Bluff	40.68	10.03	87.8	48.96	10.19	89.5
BBX 22	Bird Bluff	37.66	9.06	88.1	48.30	10.26	89.4

## References

Boyd F. R. and Mertzman S. A. (1987) Composition of structure of the Kaapvaal lithosphere, southern Africa. In *Magmatic Processes – Physicochemical Principles*, vol. 1 (ed. B. O. Mysen). The Geochemical Society, Special Publication.

Handler, M.R., Bennett, V.C., Esat, T.M., 1997. The persistence of off-cratonic lithospheric mantle: Os isotopic systematics of variably metasomatised southeast Australian xenoliths. *Earth Plan- et. Sci. Lett.* 151, 61–75.

Handler, M.R., Wysoczanski, R.J., Gamble, J.A., 2003. Proterozoic lithosphere in Marie Byrd Land, West Antarctica: Re-Os systematics of spinel peridotite xenoliths. *Chemical Geology* 196, 131-145.

Hassler, D.R., Shimizu, N., 1998. Osmium isotopic evidence for ancient subcontinental lithospheric mantle beneath the Kergue- len Islands, southern Indian Ocean. *Science* 280, 418–421.

Lawver, B.E., Royer, J.Y., Sandwell, D.T., Scotese, C.R., 1991. Evolution of the Antarctic continental margins. In: Thomson, M.R.A., Crame, J.A., Thomson, J.W. (Eds.), *Geological Evolution of Antarctica— Proceedings of the 5th International Symposium on Antarctic Earth Sciences*. Cambridge Univ. Press, Cambridge, pp. 533– 539.

Liu, J., Rudnick, R.L., Walker, R.J., Gao, S., Wu, F., Piccoli, 2010. Processes controlling highly siderophile element fractionations in xenolithic peridotites and their influence on Os isotopes. *Earth and Planetary Science Letters* 297, 287-297.

Liu, J., Rudnick, R.L., Walker, R.J., Gao, S., Wu, F., Piccoli, P.M., Yuan, H., Xu, W., Xu, Y., 2011. Mapping lithospheric boundaries using Os isotopes of mantle xenoliths: An example from the North China Craton. *Geochimica et Cosmochimica Acta* 75, 3881-3902.

Liu, J., Carlson, R.W., Rudnick, R.L., Walker, R.J., Gao, S., Wu, F., 2012. Comparative Sr-Nd-Hf-Os-Pb isotope systematics of xenolithic peridotites from Yangyuan, North China Craton: Additional evidence for a Paleoproterozoic age. *Chemical Geology* 332, 1-14.

Mukasa, S.B., Dalziel, I.W.D., 2000. Marie Byrd Land, West Antarctica: evolution of Gondwana's Pacific margin constrained by zircon U–Pb geochronology and feldspar common-Pb isotopic compositions. *Geol. Soc. Amer. Bull.* 112, 611 –627.

Pankhurst, R.J., Weaver, S.d., Bradshaw, J.D., Storey, B.C., Ireland, T.R., 1998. Geochronology and geochemistry of pre-Jurassic superterrane in Maire Byrd Land, Antarctica. *Journal of Geophysical Research.* 103, 2529-2547.

Pearson, D.G., Carlson, R.W., Shirey, S.B., Boyd, F.R., Nixon, P.H., 1995a. The stabilisation of Archaean lithospheric mantle: a Re–Os isotope study of peridotite xenoliths from the Kaapvaal and Siberian cratons. *Earth Planet. Sci. Lett.* 134, 341 – 357.

Reisberg, L.C., Lorand, J.P., 1995. Longevity of sub-continental mantle lithosphere from osmium isotopic systematics in orogen- ic peridotite massifs. *Nature* 376, 159–162.

Rudnick, R.L., Walker, R.J., 2009. Interpreting ages from Re-Os isotopes in peridotites. *Lithos* 112, 1283–1095.

Storey, B.C., Leat, P.T., Weaver, S.D., Pankhurst, R.J., Bradshaw, J.D., Kelley, S., 1999. Mantle plumes and Antarctic–New Zealand rifting: evidence from mid-Cretaceous mafic dykes. *J. Geol. Soc. (Lond.)* 156, 659–671.

Walker, R.J., Carlson, R.W., Shirey, S.B., Boyd, F.R., 1989. Os, Sr, Nd and Pb isotope systematics of southern African peridotite xenoliths: implications for the chemical evolution of subcontinental mantle. *Geochim. Cosmochim. Acta* 53, 1583 – 1595.

Wysoczanski, R.J., Gamble, J.A., Kyle, P.R., Thirlwall, M.F., 1995. The petrology of lower crustal xenoliths from the Executive Committee Range, Marie Byrd Land volcanic province, West Antarctica. *Lithos* 36, 185–201.